

W-Band Waveguide Bandpass Filters Fabricated by Micro Laser Sintering

Salek, Milan; Shang, Xiaobang; Roberts, Robert C.; Lancaster, Michael J.; Boettcher, Falko; Weber, Daniel; Starke, Thomas

DOI:

[10.1109/TCSII.2018.2824898](https://doi.org/10.1109/TCSII.2018.2824898)

Document Version

Peer reviewed version

Citation for published version (Harvard):

Salek, M, Shang, X, Roberts, RC, Lancaster, MJ, Boettcher, F, Weber, D & Starke, T 2018, 'W-Band Waveguide Bandpass Filters Fabricated by Micro Laser Sintering', *IEEE Transactions on Circuits and Systems II: Express Briefs*. <https://doi.org/10.1109/TCSII.2018.2824898>

[Link to publication on Research at Birmingham portal](#)

Publisher Rights Statement:

(c) 2018 IEEE. Personal use of this material is permitted. Permission from IEEE must be obtained for all other users, including reprinting/republishing this material for advertising or promotional purposes, creating new collective works for resale or redistribution to servers or lists, or reuse of any copyrighted components of this work in other works

Published in IEEE Transactions on Circuits and Systems II: Express Briefs on 12/03/2018

DOI: 10.1109/TCSII.2018.2824898

General rights

Unless a licence is specified above, all rights (including copyright and moral rights) in this document are retained by the authors and/or the copyright holders. The express permission of the copyright holder must be obtained for any use of this material other than for purposes permitted by law.

- Users may freely distribute the URL that is used to identify this publication.
- Users may download and/or print one copy of the publication from the University of Birmingham research portal for the purpose of private study or non-commercial research.
- User may use extracts from the document in line with the concept of 'fair dealing' under the Copyright, Designs and Patents Act 1988 (?)
- Users may not further distribute the material nor use it for the purposes of commercial gain.

Where a licence is displayed above, please note the terms and conditions of the licence govern your use of this document.

When citing, please reference the published version.

Take down policy

While the University of Birmingham exercises care and attention in making items available there are rare occasions when an item has been uploaded in error or has been deemed to be commercially or otherwise sensitive.

If you believe that this is the case for this document, please contact UBIRA@lists.bham.ac.uk providing details and we will remove access to the work immediately and investigate.

W-Band Waveguide Bandpass Filters Fabricated by Micro Laser Sintering

Milan Salek, Xiaobang Shang, *Member, IEEE*, Robert C. Roberts, *Member, IEEE*, Michael J. Lancaster, *Senior Member, IEEE*, Falko Boettcher, Daniel Weber and Thomas Starke

Abstract— This paper presents a fifth-order W-band waveguide bandpass filter with a Chebyshev response, operating at center frequency of 90 GHz and having fractional bandwidth of 11%. The filter is fabricated by micro laser sintering process which is a powder bed based additive manufacturing technology. Use of this technology allows the filter to be made accurately with high resolution and good surface quality in one piece. This results in better performance in term of insertion loss and reproducibility. For the purpose of comparison, two similar filters are presented in this paper with the same structure and specification, one made from stainless steel and the other made from stainless steel coated with copper. Both filters are tested and have excellent agreement between measurements and simulations.

Index Terms—3-D printing, Micro laser sintering process, Stereolithography, W-band, Waveguide bandpass filter.

I. INTRODUCTION

Using additive manufacturing technologies to fabricate microwave components has become of interest in recent years. Both metallic and non-metallic materials are used in additive manufacturing fabrication processes, but non-metallic materials generally need to be coated with a conductive layer using a surface metallization process to achieve a good electrical conductivity.

Manuscript received January 12, 2018; accepted February 12, 2018. Date of publication March 12, 2018; date of current version April 12, 2018. The project was supported by the U.K. Engineering and Physical Science Research Council (EPSRC) under contract EP/M016269/1, 3D Micro Print GmbH in Germany and Additive Microfabrication Laboratory of The University of Hong Kong.

M. Salek and M. J. Lancaster are with the Department of Electronic, Electrical and Systems Engineering, University of Birmingham, Birmingham B15 2TT, U.K. (e-mail: mxs1149@bham.ac.uk; m.j.lancaster@bham.ac.uk).

X. Shang was with the Department of Electronic, Electrical and Systems Engineering, University of Birmingham, U.K. He is now with National Physical Laboratory, Middlesex TW11 0LW, U.K. (e-mail: xiaobang.shang@npl.co.uk).

R. C. Roberts is with Department of Computer Science, University of Hong Kong, Hong Kong. (e-mail: rcr8@hku.hk).

D. Weber was with 3D Micro Print GmbH, Chemnitz 09126, Germany. He is now with Freeman Technology, Tewkesbury GL20 8DN U.K. (e-mail: engineering.daniel.weber@gmail.com).

F. Boettcher and T. Starke are with 3D Micro Print GmbH, Chemnitz 09126, Germany. (e-mail: falko.boettcher@3dmicroprint.com; thomas.starke@3dmicroprint.com).

Color versions of one or more of the figures in this paper are available online at <http://ieeexplore.ieee.org>.

Digital Object Identifier.

Using additive technologies allows components with complex structure to be fabricated at low cost with high accuracy. Many different types of additive manufacturing technologies are available such as stereolithography apparatus (SLA), fused deposition modelling (FDM) and selective laser sintering (SLS) [1]. Fabrication of microwave filters operating at both low and high frequencies (0.5 GHz to 100 GHz) using the stereolithography-based 3-D printing technique is well proven to work with good results as shown in [1]-[11]. Other microwave components produced by stereolithography-based 3-D printing are antennas with examples reported in [12]-[16].

Stereolithography-based 3-D printing makes use of photodefinable plastic materials; so printed filters must be subsequently coated with conductive materials using surface metallization process. This results in an increase in complexity of the fabrication process and cost. However, using the micro laser sintering process allows metallic materials to be used directly. Using a metallic fabrication process increases the strength of components, as well as insuring wider working temperature range and better thermal expansion properties.

This paper describes a W-band waveguide bandpass filter, which is fabricated by micro laser sintering, also known as selective laser sintering or selective laser melting. Using this technique allows the filter to be manufactured with high accuracy, high resolution and good surface quality.

The filter reported here operates at center frequency of 90 GHz with bandwidth of 10 GHz, and to the best of author's knowledge this is the highest frequency filter fabricated by micro laser sintering process. The waveguide bandpass filter design is reasonably conventional, using coupling matrix theory to design a filter based on five rectangular resonators which are coupled using inductive irises [17, 18]. In addition to the waveguide filter, the standard UG387/U flange was included in the fabrication process enabling accurate connection to measurement system.

There are many different types of conductive powder materials that are commonly used in the micro laser sintering process such as stainless steel, molybdenum and tungsten. Stainless steel used in fabrication process of both filters with one being coated with copper to compare insertion loss.

II. BANDPASS FILTER DESIGN

The filter is constructed with five coupled rectangular resonators operating in the TE₁₀₁ mode. The couplings between the resonators as well as input/ output coupling are

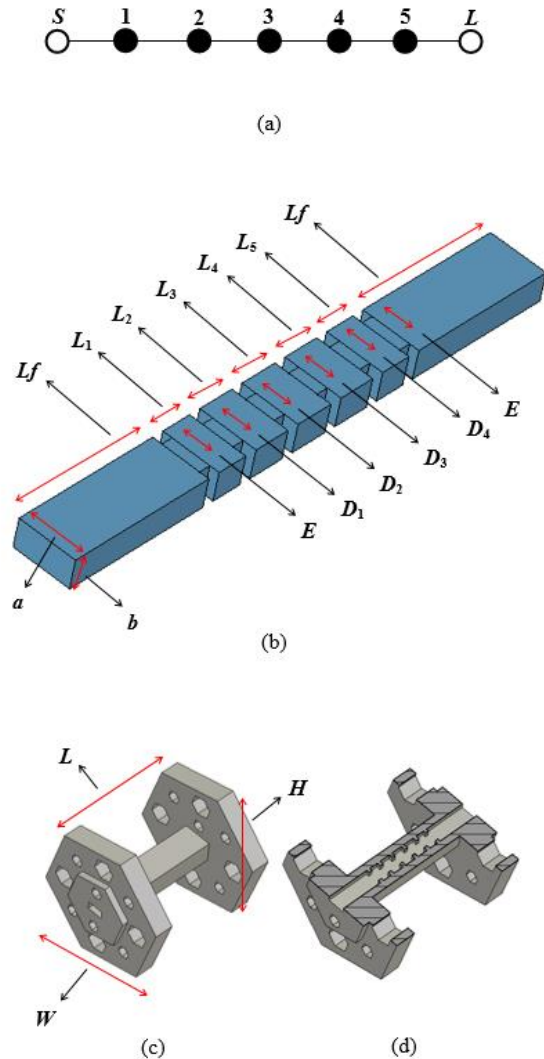


Fig. 1. Illustration of the fifth-order waveguide bandpass filter. (a) Coupling routing diagram of the filter. (b) Internal structure of the filter showing internal dimensions. The dimensions in millimeter are: $L_f=6.48$, $L_1=L_5=1.317$, $L_2=L_4=1.582$, $L_3=1.636$, $E=1.7$, $D_1=D_4=1.374$, $D_2=D_3=1.291$, $a=2.54$ and $b=1.27$. (c) Completed filter, showing external dimensions. The dimensions in millimeter are: $L=21.4$, $H=19.05$ and $W=22$. (d) A cross section view of the filter showing internal couplings between resonators.

realized using inductive irises. The filter is specified in terms of the Chebyshev bandpass response with center frequency of 90 GHz, bandwidth of 10 GHz (fractional bandwidth of 11%) and return loss of 20 dB over the passband. Using coupling matrix theory [17], the filter specification is translated into coupling matrix elements, which are then translated into physical dimensions according to the procedure in [17, 18].

A coupling routing diagram of the filter can be seen in Fig. 1 (a). The un-normalized non-zero coupling coefficients between resonators are $M_{12}=M_{45}=0.0961$, $M_{23}=M_{34}=0.0706$ and the external quality factor of the first (Q_{e1}) and the last (Q_{en}) resonators are calculated to be $Q_{e1}=Q_{en}=8.76$ [17, 18].

The physical dimensions which correspond to the coupling and Q values are found by the standard technique. Looking at

Fig. 1 (b), it can be seen that coupling between resonators is realized by the width of irises, which are denoted by $D_1=D_4$ and $D_2=D_3$ and set by coupling coefficients $M_{12}=M_{45}$ and $M_{23}=M_{34}$ respectively. The input/ output coupling is realized by adjusting the width of the iris denoted by E , which is set by external quality factors $Q_{e1}=Q_{en}$. Simulations and final optimization of the filter are carried out in CST Microwave Studio [19] to get the frequency response close to the ideal.

Fig. 1 (c) illustrates the external design of the W-band waveguide bandpass filter, along with its external dimensions in millimeters. Fig. 1 (d) shows a cross section view of the filter with the resonators and all internal couplings between resonators shown. The screw holes, alignment pin holes and precision alignment pin holes are included in both input and output UG387/U waveguide flanges. The filter and flange are designed in the hexagonal shape in order to facilitate fabrication by the micro laser sintering process.

III. MICRO LASER SINTERING FABRICATION PROCESS

Micro laser sintering is an additive manufacturing process, which is by far the most accurate sintering fabrication process to 3D print solid metal structures. Using the micro laser sintering process enables parts with complex 3D micro structures to be produced at reasonable costs, where conventional additive manufacturing processes reach their limits. In the process the model structure is divided into layers, and each layer is printed by applying a thin layer of metal powder to a build platform and then, using a laser beam, the powder is selectively fused according to the required layer structure. Once a layer is constructed, the building platform is lowered, and next layer will be constructed with same process as in previous layers. The process continues until all layers are constructed on top of each other according to 3D model structure [20]. The accuracy of micro laser sintering makes this fabrication process attractive for fabricating high frequency waveguide filters, as it enables the production of small filters with complex structures and high strength.

Two similar filters with the same structure and specification were made to compare insertion loss. Both filters made from stainless steel with one being coated with copper. The filters were fabricated by 3D Micro Print GmbH [20], using their micro laser sintering process in an inert argon atmosphere. The laser source was an IR fiber laser with a 50 W laser average power. The laser spot diameter is focused down to 30 μm and was operated in continuous wave mode. The filters are made from stainless steel powder material with one being coated with a 5 μm thick copper layer by electroplating the surface. The type of stainless steel was 1.4542 (17-4PH) according to ASTM 564, which is a chromium nickel copper alloyed stainless steel, containing 17% chromium, 4% nickel, 4% copper and 0.3% niobium. The powder particle sizes were smaller than d_{80} 5 μm and had electrical conductivity of 1.25×10^7 S/m. The thickness of each layer in the process was set at 5 μm . The print took about 16 hours, but this could be considerably reduced by optimizing the build process further.

Fig. 2 (a) shows photograph of the filter on the support structure after fabrication. Fig. 2 (b) provides a photograph of

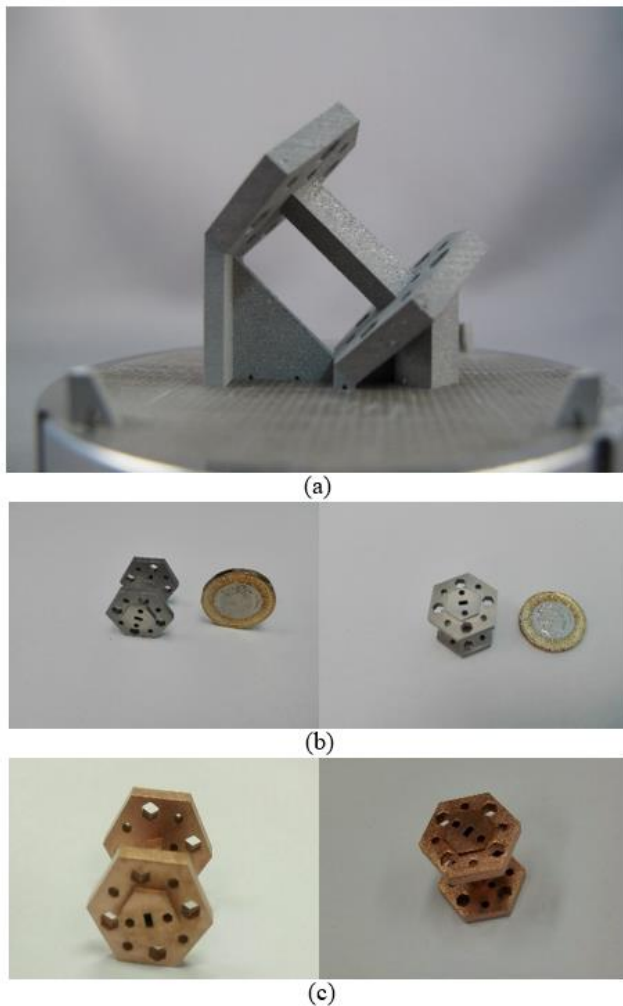


Fig. 2. Photograph of the fabricated W-band waveguide bandpass filter. (a) Filter on support structure after fabrication process. (b) Fabricated filter made from stainless steel. (c) Fabricated filter made from stainless steel, coated with copper.

the fabricated filter made from Stainless Steel and Fig. 2 (c) shows the fabricated filter made from stainless steel after being electroplated with $5\mu\text{m}$ thick copper layer with electrical conductivity of $5.96 \times 10^7 \text{ S/m}$.

IV. MEASUREMENT AND DISCUSSION

The S -parameter measurements of both filters are performed on Keysight E8361C PNA network analyzer. Fig. 3 shows photograph of the measurement setup. Here the filter is placed between two waveguide flanges of the network analyzer, aligned using four precision alignment pins of the waveguide flanges and tightened using four screws on each side. Fig. 4 and Fig. 5 show the measured and simulated results of both W-band waveguide bandpass filters, where the measured results are denoted with solid lines and simulated results with dashed lines. Looking at the stainless steel filter in Fig. 4 (a), it can be seen that the measured center frequency, shifts down by 1.66 GHz and a minimum return loss of 24.41 dB across the whole passband. Looking at the copper coated filter in Fig. 5 (a), it can be observed that the frequency shift is only 0.9 GHz and a minimum return loss of 26.56 dB across the

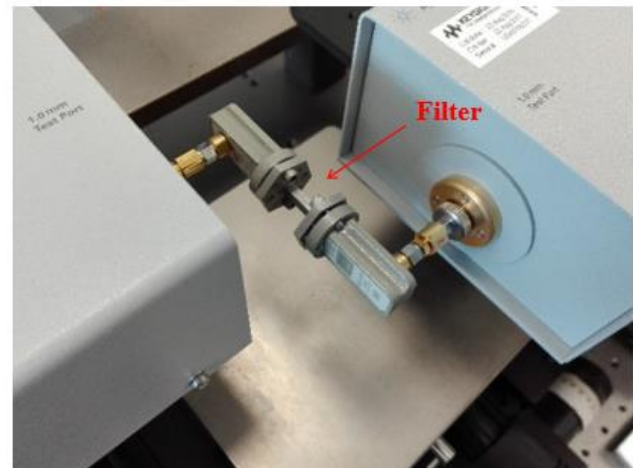


Fig. 3. Photograph of the measurement setup with the filter being placed between two waveguide flanges of the network analyzer.

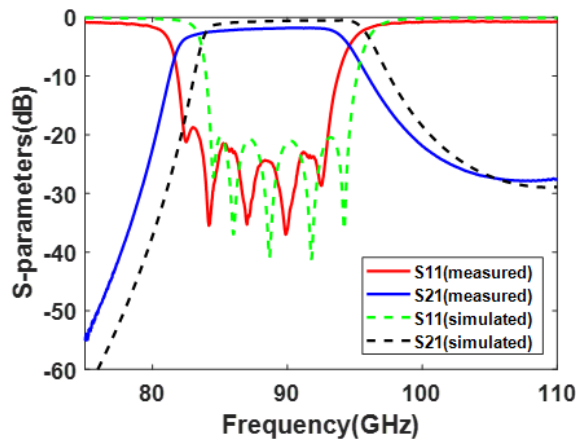
whole passband. The lower return loss of 15.2 dB at 84.6 GHz in Fig. 5 (a) is caused by slight deviation of the cavity sizes from the design and can be improved by tuning filter. To be clear, there has been no tuning of the filters and these excellent responses show the high quality of the 3D printing.

The unwanted frequency shifts in the filters is believed to be caused by small dimensional inaccuracies, as a result of expansion in length of resonators, which could be corrected by remanufacturing. It has been found that such an expansion of dimensions is repeatable and as both filters have small frequency shift, the model could be adjusted accordingly to compensate during the remanufacturing.

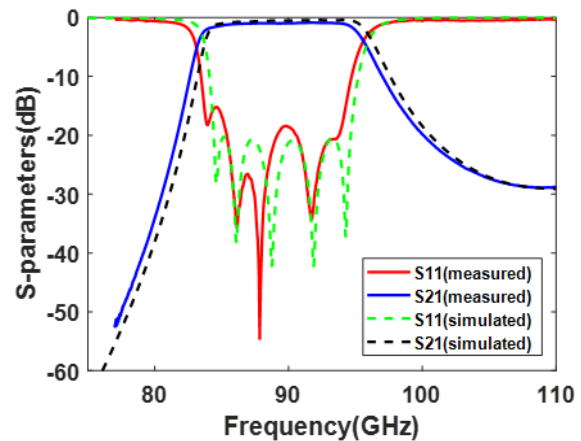
Careful examination of the expanded view of S_{21} in Fig. 4 (b) shows an average insertion loss of around 1.94 dB over the passband for the measured results, which is 1.34 dB higher than the simulated results. The expanded view of S_{21} in Fig. 5 (b) shows an average insertion loss of around 1 dB over the passband for the measured results, which is 0.47 dB higher than simulated results. Note, the copper plated filter has 0.94 dB lower measured insertion loss in comparison to the filter made from stainless steel showing the advantages of the copper coating.

The typical surface roughness values of the filters measured with Mitutoyo SurfTest SV-3000 CNC surface roughness tester is about $2 \mu\text{m}$. This reduces effective conductivity of stainless steel to $3.19 \times 10^6 \text{ S/m}$ and copper to $14.97 \times 10^6 \text{ S/m}$. According to calculations [19] this results in additional loss of 0.456 dB for the filter that is not coated with copper and 0.453 dB for the copper coated filter, however this loss is already reflected in the CST simulated results. The loss in the waveguide jointing the filter to the flanges (0.075dB) is also included in the simulations. In addition, small misalignments during measurements also contribute to the difference in insertion loss but show up in the return loss. The 20 dB return loss contributes about 0.1 dB to the insertion loss.

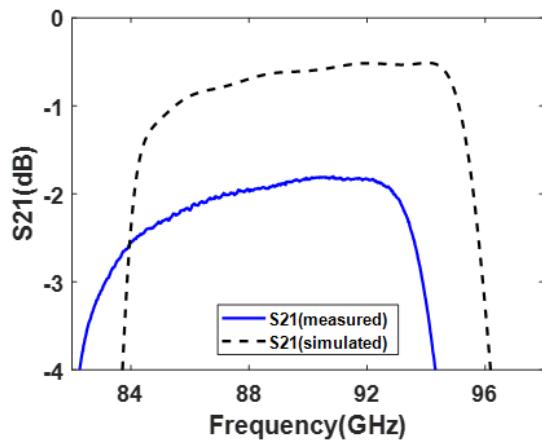
The additional difference in insertion loss between simulation and measurement is probably caused by a combination of factors including the estimate of the conductivity of the stainless steel and copper which may not



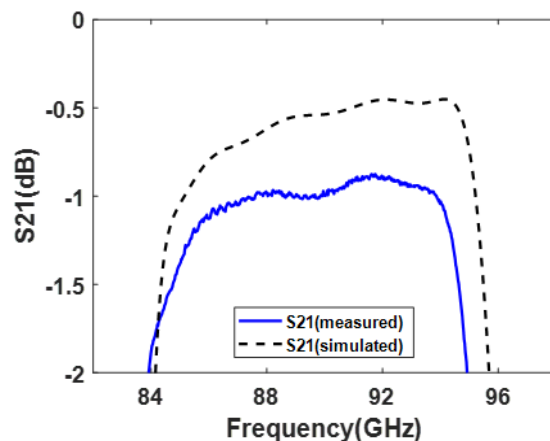
(a)



(a)



(b)



(b)

Fig. 4. Measured and simulated results of the W-band waveguide bandpass filter made from stainless steel. (a) Measured and simulated results over the whole W-band. (b) Expanded view of S_{21} over passband.

Fig. 5. Measured and simulated results of the W-band waveguide bandpass filter made from stainless steel coated with $5\mu\text{m}$ thick copper layer. (a) Measured and simulated results over the whole W-band. (b) Expanded view of S_{21} over passband.

be as specified due to impurities, surface contaminates, or oxidation. There may be effects because of the granular nature of the surface formed from the powder as well as changes from the specified stainless steel conductivity because of the manufacturing process. Because of the high frequency and the small skin depth, the loss is highly dependent on these surface effects. A further detailed study is required here to understand these losses. The insertion loss can be improved by electroplating the surface (as we have seen), laser polishing, chemical polishing and using higher conductivity powder materials.

Table I provides a comparison of measured performance of waveguide bandpass filters that are fabricated using different types of manufacturing technique.

V. CONCLUSION

A metal 3D printed W-band waveguide bandpass filter fabricated by micro laser sintering process has been presented in this paper. This is the highest frequency metal 3D printed filter so far reported. Good agreement between the measured and simulated results demonstrate that micro laser sintering process can be used to fabricate filters with complex

structures, that operate at high frequencies accurately. The micro laser sintering technique not only offers accuracy, but it also enables the whole structure, including flanges, to be made in a single piece. In addition, using electroplated copper demonstrates, it can improve the insertion loss of the filter considerably.

REFERENCES

- [1] M. Dauria, W. J. Otter, J. Hazell, B. T. W. Gillatt, C. Long-Collins, N. M. Ridler, and S. Lucyszyn, "3-D Printed Metal-Pipe Rectangular Waveguides," *IEEE Transactions on Components, Packaging and Manufacturing Technology*, vol. 5, no. 9, pp. 1339–1349, 2015.
- [2] X. Shang, J. Li, C. Guo, M. J. Lancaster, and J. Xu, "3-D printed filter based on helical resonators with variable width," *2017 IEEE MTT-S International Microwave Symposium (IMS)*, 2017.
- [3] C. Guo, J. Li, J. Xu, and H. Li, "An X-band lightweight 3-D printed slotted circular waveguide dual-mode bandpass filter," *2017 IEEE International Symposium on Antennas and Propagation & USNC/URSI National Radio Science Meeting*, 2017.
- [4] L. Araujo, X. Shang, M. Lancaster, A. D. Oliveira, I. Llamas-Garro, J.-M. Kim, M. Favre, M. Billod, and E. D. Rijk, "3-D printed band-pass combline filter," *Microwave and Optical Technology Letters*, vol. 59, no. 6, pp. 1388–1390, 2017.
- [5] C. Guo, X. Shang, M. J. Lancaster, and J. Xu, "A 3-D Printed Lightweight X-Band Waveguide Filter Based on Spherical

TABLE I
COMPARISON WITH OTHER WAVEGUIDE BANDPASS FILTERS

| f_c (GHz) | FBW | IL (dB) | RL (dB) | Manufacturing techniques | f_c offset | Reference |
|-------------|--------|----------|---------|--------------------------|--------------|------------------------|
| 107.2 | 6.34% | 0.95 | >11 | SLA | 7.2% | [1] |
| 100 | 4% | 0.5~0.8 | >15 | Laser micromachining | 0% | [10] |
| 87.5 | 11.5% | 0.3~0.5 | >18 | SLA | 2.78% | [10] |
| 88.47 | 9.7% | 0.97~1.1 | >15 | SU-8 process | 1.7% | [21] |
| 102 | 5% | 1.2 | >10 | SU-8 process | 2% | [22] |
| 100 | 10% | 0.6 | >18 | CNC milling | 0% | [23] |
| 92.6 | 4.53% | 0.5 | >14 | CNC milling | 0.02% | [24] |
| 92.45 | 4.83% | 1.1~1.3 | >10 | DRIE | 1.86% | [25] |
| 95 | 3.68% | 3.49 | >18 | Hot embossing | 0.52% | [26] |
| 75.5 | 5.3% | 8 | >8 | SLM | 2.72% | [27] |
| 88.34 | 12.1% | 1.94 | >18 | MLS | 1.84% | T.W. (stainless steel) |
| 89.1 | 11.07% | 1 | >15 | MLS | 1% | T.W. (copper coated) |

f_c : center frequency of the filter; FBW: fractional bandwidth; IL: passband insertion loss; RL: passband return loss; f_c offset: frequency shift; T.W.: this work.

Resonators,” *IEEE Microwave and Wireless Components Letters*, vol. 25, no. 7, pp. 442–444, 2015.

[6] C. Guo, X. Shang, J. Li, F. Zhang, M. J. Lancaster, and J. Xu, “A Lightweight 3-D Printed X-Band Bandpass Filter Based on Spherical Dual-Mode Resonators,” *IEEE Microwave and Wireless Components Letters*, vol. 26, no. 8, pp. 568–570, 2016.

[7] C. Guo, J. Li, D. D. Dinh, X. Shang, M. J. Lancaster, and J. Xu, “Ceramic filled resin based 3D printed X-band dual-mode bandpass filter with enhanced thermal handling capability,” *Electronics Letters*, vol. 52, no. 23, pp. 1929–1931, Oct. 2016.

[8] J. Li, C. Guo, L. Mao, and J. Xu, “Compact high-Q hemispherical resonators for 3-D printed bandpass filter applications,” *2017 IEEE MTT-S International Microwave Symposium (IMS)*, 2017.

[9] J. Li, C. Guo, J. Xu, and L. Mao, “Lightweight low-cost Ka-band 3-D printed slotted rectangular waveguide bandpass filters,” *2017 IEEE International Symposium on Antennas and Propagation & USNC/URSI National Radio Science Meeting*, 2017.

[10] X. Shang, P. Penchev, C. Guo, M. J. Lancaster, S. Dimov, Y. Dong, M. Favre, M. Billod, and E. D. Rijk, “W-Band Waveguide Filters Fabricated by Laser Micromachining and 3-D Printing,” *IEEE Transactions on Microwave Theory and Techniques*, vol. 64, no. 8, pp. 2572–2580, 2016.

[11] G. Venanzoni, M. Dionigi, C. Tomassoni, D. Eleonori, and R. Sorrentino, “3D printing of X band waveguide resonators and filters,” *2017 XXXIInd General Assembly and Scientific Symposium of the International Union of Radio Science (URSI GASS)*, 2017.

[12] M. V. D. Vorst and J. Gumpinger, “Applicability of 3D printing techniques for compact Ku-band medium/high-gain antennas,” *2016 10th European Conference on Antennas and Propagation (EuCAP)*, 2016.

[13] F. Bongard, M. Gimersky, S. Doherty, X. Aubry, and M. Krummen, “3D-printed Ka-band waveguide array antenna for mobile SATCOM applications,” *2017 11th European Conference on Antennas and Propagation (EUCAP)*, 2017.

[14] K. F. Brakora, J. Halloran, and K. Sarabandi, “Design of 3-D Monolithic MMW Antennas Using Ceramic Stereolithography,” *IEEE Transactions on Antennas and Propagation*, vol. 55, no. 3, pp. 790–797, 2007.

[15] B. Liu, X. Gong, and W. Chappell, “Applications of Layer-by-Layer Polymer Stereolithography for Three-Dimensional High-Frequency Components,” *IEEE Transactions on Microwave Theory and Techniques*, vol. 52, no. 11, pp. 2567–2575, 2004.

[16] J. S. Silva, E. B. Lima, J. R. Costa, C. A. Fernandes, and J. R. Mosig, “Tx-Rx Lens-Based Satellite-on-the-Move Ka-Band Antenna,” *IEEE Antennas and Wireless Propagation Letters*, vol. 14, pp. 1408–1411, 2015.

[17] R. J. Cameron, C. M. Kudsia, and R. R. Mansour, *Microwave filters for communication systems: fundamentals, design and applications*. Hoboken, NJ, USA: Wiley, 2007.

[18] J.-S. Hong, *Microstrip filters for RF/microwave applications*. Hoboken, NJ: John Wiley & Sons, 2011.

[19] Computer Simulated Technology (CST), *Microwave Studio*, 2017. Available at <http://www.cst.com/>.

[20] 3D Micro Print GmbH. [Online]. Available: <http://www.3dmicroprint.com/>.

[21] X. Shang, M. Ke, Y. Wang, and M. Lancaster, “Micromachined W-band waveguide and filter with two embedded H-plane bends,” *IET Microwaves, Antennas & Propagation*, vol. 5, no. 3, p. 334, 2011.

[22] C. A. Leal-Sevillano, J. R. Montejo-Garai, M. Ke, M. J. Lancaster, J. A. Ruiz-Cruz, and J. M. Rebolgar, “A Pseudo-Elliptical Response Filter at W-Band Fabricated With Thick SU-8 Photo-Resist Technology,” *IEEE Microwave and Wireless Components Letters*, vol. 22, no. 3, pp. 105–107, 2012.

[23] C. A. Leal-Sevillano, J. R. Montejo-Garai, J. A. Ruiz-Cruz, and J. M. Rebolgar, “Low-Loss Elliptical Response Filter at 100 GHz,” *IEEE Microwave and Wireless Components Letters*, vol. 22, no. 9, pp. 459–461, 2012.

[24] X. Liao, L. Wan, Y. Zhang, and Y. Yin, “W-band low-loss bandpass filter using rectangular resonant cavities,” *IET Microwaves, Antennas & Propagation*, vol. 8, no. 15, pp. 1440–1444, Sep. 2014.

[25] Y. Li, P. Kirby, and J. Papapolymerou, “Silicon Micromachined W-Band Bandpass Filter Using DRIE Technique,” *2006 European Microwave Conference*, 2006.

[26] F. Sammoura, Y. Cai, C.-Y. Chi, T. Hirano, L. Lin, and J.-C. Chiao, “A micromachined W-band iris filter,” *The 13th International Conference on Solid-State Sensors, Actuators and Microsystems, 2005. Digest of Technical Papers. TRANSDUCERS 05.*, 2005.

[27] B. Zhang and H. Zirath, “3D printed iris bandpass filters for millimetre-wave applications,” *Electronics Letters*, vol. 51, no. 22, pp. 1791–1793, 2015.